Applied Numerical Modeling in Geomechanics – 2020 – Billaux, Hazzard, Nelson & Schöpfer (eds.) Paper: 17-01
©2020 Itasca International, Inc., Minneapolis, ISBN 978-0-9767577-5-7

Tunneling underneath a heritage-listed building in the heart of Sydney

J. Rabanser[1], C.J. Wang[2] & H. Lagger[1]
[1]*Arup, London, United Kingdom*
[2]*Arup, Sydney, Australia*

1 INTRODUCTION

This paper focuses on the design of a tunnel beneath a heritage-listed building in the heart of Sydney, Australia. Numerical analysis using *3DEC* (Itasca 2016) were carried out. For the performed analysis, a stochastic discrete fracture network (DFN) approach has been applied and the numerical results are compared to manually generated fractures based on published data. Fracture intensity, block size distribution and tunnel crown displacements serve as the comparison criteria between the two methods.

2 GROUND CONDITIONS

The site is set within the Hawkesbury Sandstone of the Sydney Basin in New South Wales, Australia. The Hawkesbury Sandstone has been described by Pells (2004) as Triassic-aged medium to coarse-grained quartz sandstone comprising of sheet and massive facies with minor mudstone lenses. Sedimentary rocks within the Sydney basin have been classified by Pells et al. (1998) into Sandstone and Shale Classes (Classes I to V) to group rocks exhibiting similar engineering properties and behavior. Based on available ground investigation data, the site stratigraphy in the upper 10m consists of Class IV Sandstone followed by a 15m-thick Class III Sandstone overlying the Class II Sandstone. Major discontinuities include, as identified, the bedding and two joint sets. The joint sets have been described as orthogonal sub-vertical defects, which are orientated towards NNE and ESE.

It is well recognized that the virgin in-situ stress field in the Sydney Basin comprises of high horizontal stress components as a result of locked-in tectonic stress. The major horizontal stress orientation is NNE to SSW and within the area of interest approximately 2.5 times the vertical stress. These high horizontal stresses strongly influence the excavation-induced ground movements due to the undertaken tunneling works.

3 DEVELOPMENT OF DFN

The stochastic Discrete Fracture Network (DFN) model for the site is generated from a combination of nearby tunnel mapping records, borehole logs, televiewer logs and published regional geological dataset. Fracture characteristics such as orientation, aperture, persistence and termination are incorporated into the model. Fracture types include sub-horizontal bedding partings and three joint sets (two orthogonal sub-vertical sets plus a random set).

Fractures are generated using stochastic processes and follow the principles of the conventional Poisson model (Dershowitz & Einstein 1988). The lineal fracture intensity (P_{10}) inform the number of fracture seeds within each voxel (block). P_{10} for bedding partings and joint sets are randomly assigned into each voxel adhering to their probabilistic distribution of P_{10} derived from the borehole logs and televiewer data.

Joint types are allocated based on their probability of occurrence identified from the tunnel mapping records. Fracture orientation and persistence are simulated at each fracture seed location using a normal distribution derived from their respective statistical attributes. The generated fractures are calibrated and validated against the average areal fracture intensity (P_{21}) obtained from the tunnel mapping records. The average P_{21} of the simulated DFN is determined from randomly generated cross sections and long sections within the DFN model. The calibration process consists of cleaning fracture seeds (remove/ add) and manipulation of the fracture persistence's statistical attributes (mean, standard deviation and skewness).

Five separate model simulations were completed to ensure the model parameters are robust against the validation P_{21}. In Figure 1 the process of stochastic DFN generation and validation is pictured. The resulting DFN model is a reasonable representation of the rock discontinuity network and is designated further on as *M1: Stochastic DFN*.

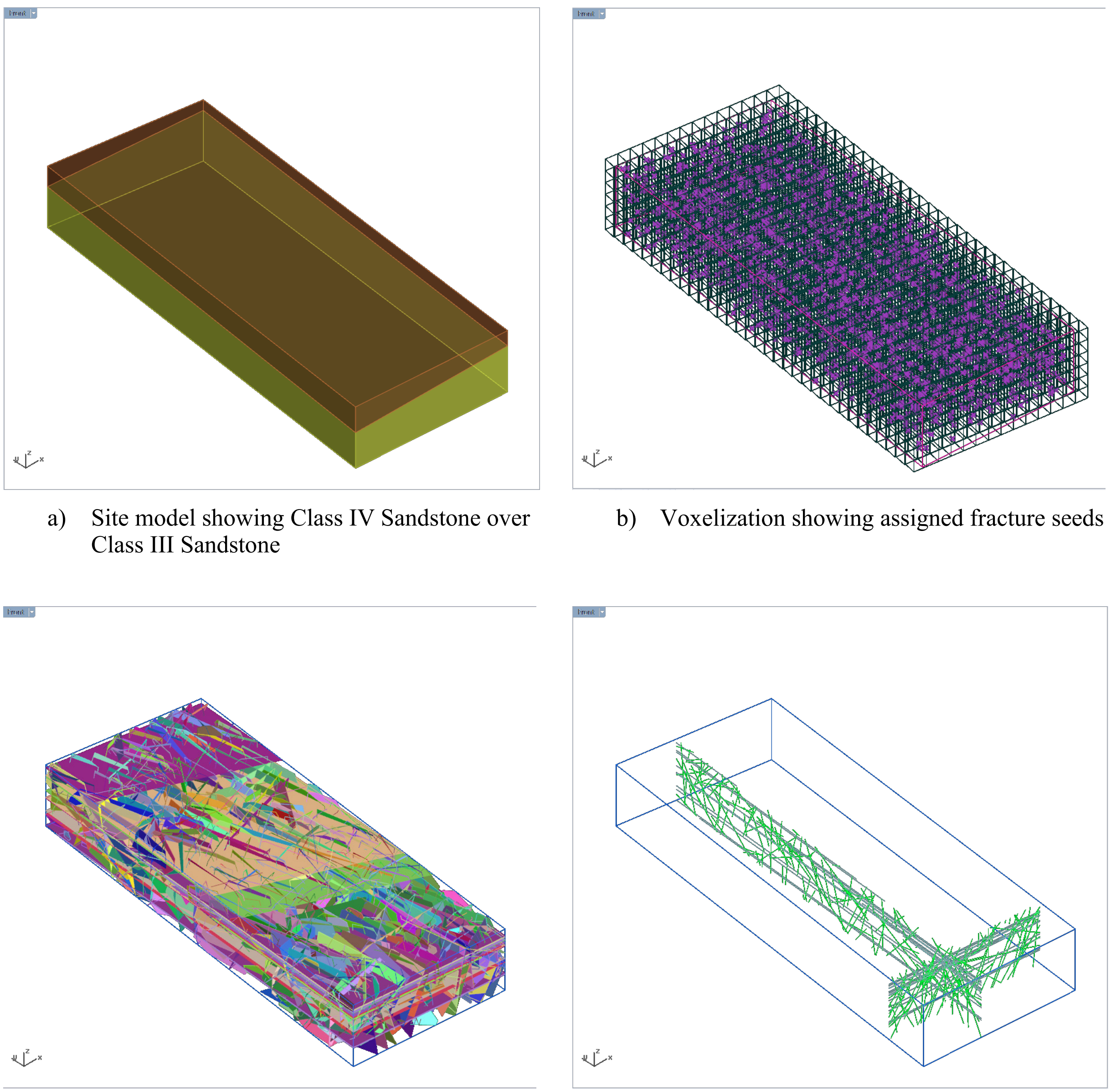

a) Site model showing Class IV Sandstone over Class III Sandstone

b) Voxelization showing assigned fracture seeds

c) 3D DFN

d) 2D DFN

Figure 1. Steps of stochastic DFN generation and validation.

4 DFN GENERATION IN *3DEC*

Two different fracture networks were generated in *3DEC*. First, the stochastically generated DFN (*M1: Stochastic DFN*) was used as a basis for fracture generation. Due to the geometric assumptions made by *3DEC*, only fully detached convex shaped blocks are possible. Therefore, concave blocks and partially split blocks (due to realistic persistence) developed by the stochastic generated reference DFN cannot be directly imported into *3DEC*. As a result, an additional workflow has been developed to generate a DFN within *3DEC* which provides a similar fracture network. A Python script was used to create for each individual reference DFN fracture a *3DEC* joint set command. To avoid fully persistent joints, a termination criterion based on volumetric fracture intensity was defined. The obtained *3DEC* DFN is designated as: *M2: 3DEC – Stochastic DFN*.

A second *3DEC* fracture network was generated manually. The *3DEC* joint set command allows to specify spacing, number of fractures, and furthermore a standard deviation for dip angle, dip direction and spacing. With this option a set of similar joints can be generated in one go. In this case fractures were generated purely based on published data of defect orientation and spacing (by Bertuzzi & Pells (2002).). To avoid fully persistent joints resulting in uniform block shapes and sizes, a standard deviation for dip angle and dip direction was applied. This manually generated fracture network is designated as: *M3: 3DEC – manually generated fractures*.

5 COMPARISON OF FRACTURE NETWORKS

Table 1 shows the comparison of fracture intensity for tunnel mapping of adjacent underground structures and three different generated fracture networks for a volume of approximately 27,000m^3.

The validation of *3DEC* fractures, generated based on the stochastically generated DFN, shows that the areal (P_{21}) and volumetric (P_{32}) fracture intensity is very similar for Class III Sandstone to the stochastic generated DFN model. For Class IV Sandstone similar volumetric fracture intensities (P_{32}) resulted in a higher areal fracture intensity (P_{21}) in *3DEC*. Since tunnel mapping data demonstrated a wide spread of areal fracture intensity values, the higher values of Class IV Sandstone were accepted. For the manually generated *3DEC* fracture network, the areal fracture intensity (P_{21}) of Class III Sandstone was slightly underestimated which is in relation with a lower volumetric fracture intensity (P_{32}). Areal fracture intensity values (P21) were calculated for multiple sections. For stochastically generated DFNs, P_{21} values showed a very narrow range, hence only the average values are specified.

Table 1. Comparison of areal (P_{21}) and volumetric (P_{32}) fracture intensities.

Model	Class	No. of Sections	P_{21} east-west	No. of Sections	P_{21} north-south	P_{32}
Tunnel Mapping (adjacent tunnels)	III	17	average: 1.70 (0.92 – 2.90)			-
	IV	26	average: 2.32 (0.72 – 4.39)			-
M1: Stochastic DFN	III	10	1.82	10	1.54	2.06
	IV	10	2.48	10	2.12	2.51
M2: *3DEC* – Stochastic DFN	III	7	1.88	3	1.71	1.96
	IV	7	3.1	3	2.76	2.57
M3: *3DEC* – manually generated fractures	III	2	1.21	2	1.19	1.39
	IV	2	2.37	2	2.02	2.33

In Figure 2 the two different fracture networks are displayed. By comparing them visually, it can be observed that the manually generated fracture network demonstrates a much lower randomness of fractures leading to blocks with a uniform shape.

By plotting block size histograms and block size distribution, as shown in Figures 3 & 4, it can be inferred that the manually generated fracture network results in a more uniform block size distribution and it highly underestimates the number of small blocks.

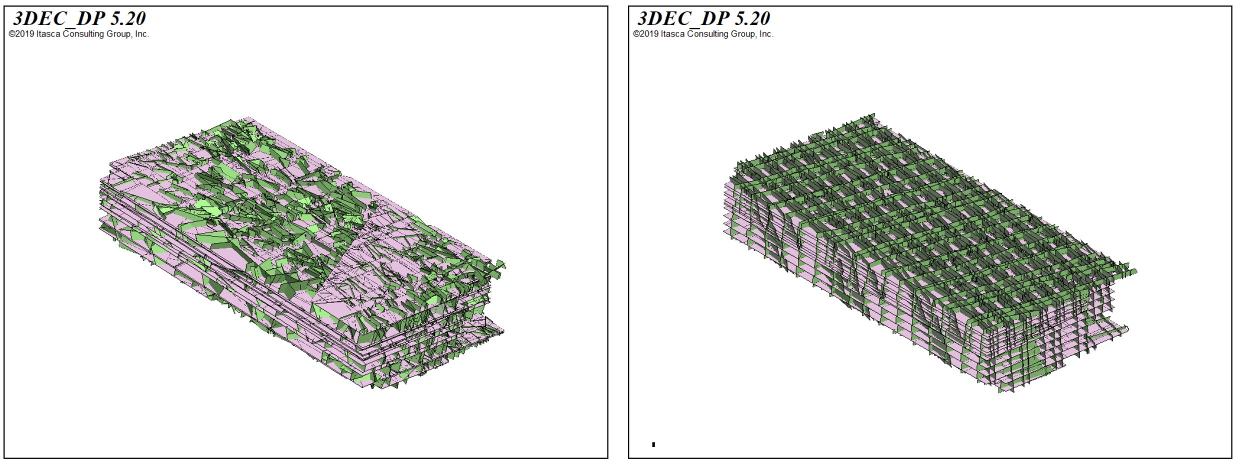

Figure 2. Analyzed fracture networks: a: M2: *3DEC* – Stochastic DFN; b: M3: *3DEC* – manually generated fractures.

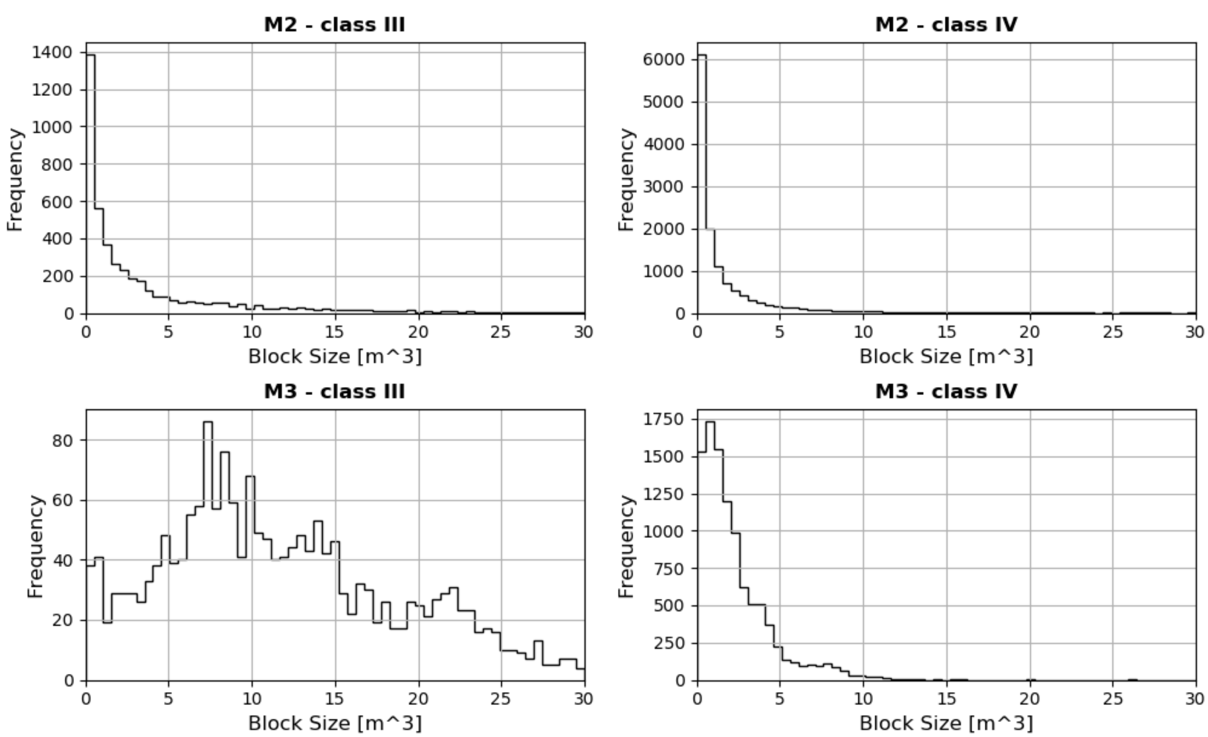

Figure 3. Block size histogram.

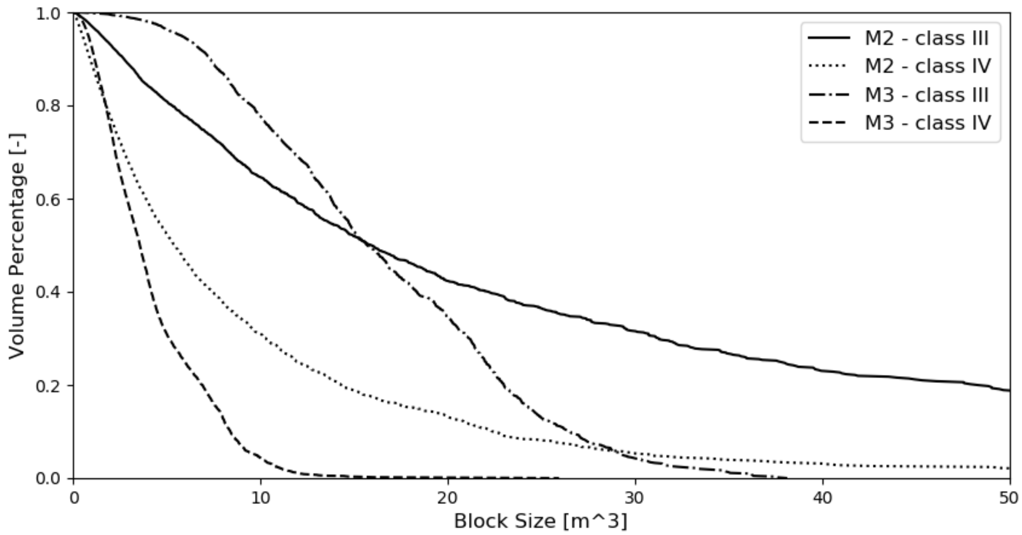

Figure 4. Block size distribution.

6 NUMERICAL ANLAYSES

The examined tunnel has a horseshoe profile and is approximately 9m wide and 6m high connecting two shafts with a shallow cover below a heritage-listed building. High concentrated loads (up to 10 MN) are expected from pad footings of the above existing building. To provide an indication of unstable blocks, all analyses were performed for an unsupported tunnel case.

In Figure 5, vertical crown displacements are plotted along the tunnel. It can be seen that the general displacement pattern is similar. Due to the higher fracture intensity the magnitude of displacements is higher by 30% for the stochastic generated DFN compared to manually generated fractures. Furthermore, this plot illustrates that potentially unstable blocks (spikes in curve) are present in the model with the stochastic generated DFN after reaching equilibrium. In the manually generated fractures model unstable blocks do not occur.

Due to the randomness of DFN generation, multiple simulations on the basis of different stochastically generated DFNs should be conducted to capture possible different scenarios. The present Paper demonstrates one of two analyzed *3DEC* model outputs. A second model shows the same magnitude of maximum crown displacements, but potentially unstable blocks occurring at different locations.

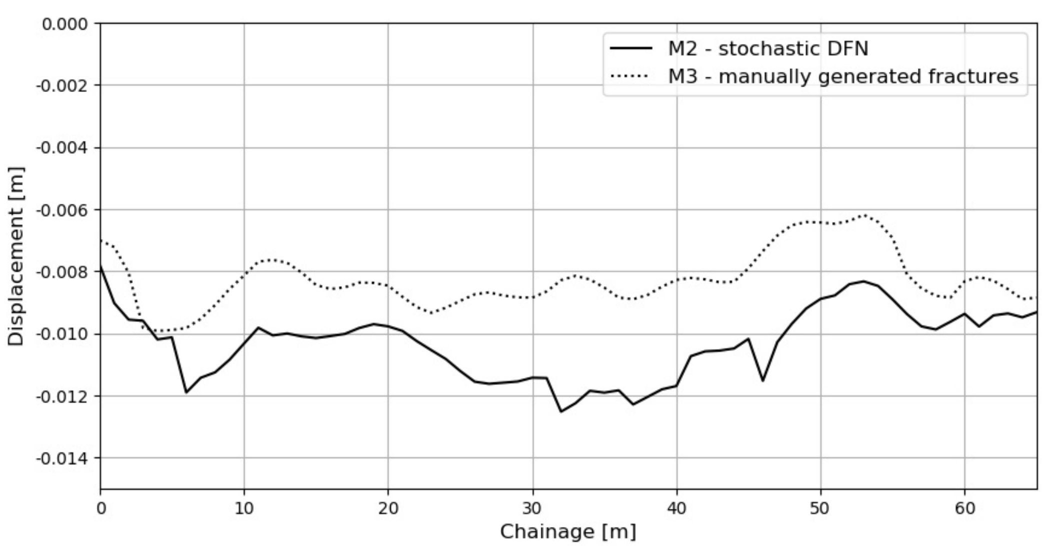

Figure 5. Comparison of vertical crown displacements along the tunnel.

7 CONCLUSIONS

This paper presents a method of incorporating a stochastic generated DFN model in *3DEC* numerical analyses. Available tunnel mapping records allowed the stochastic generated DFN to be calibrated and validated against the site-specific conditions. It was possible to demonstrate that fracture networks, generated manually in *3DEC* result in lower fracture intensities and unrealistic block size distributions, which results in less crown displacements and underestimation of unstable blocks.

REFERENCES

Dershowitz, W.S. & Einstein, H.H. 1988. Characterizing rock joint geometry with joint system models. *Roc Mechanics and Rock Engineering*, 21(1), 21-51.

Bertuzzi R. & Pells P.J.N. 2002. Geotechnical Parameters of Sydney sandstone and shale. *Australian Geomechanics*, Vol 37, No. 5 December 2002.

Bertuzzi R. 2014. Sydney sandstone and shale parameters for tunnel design. *Australian Geomechanics*, Vol 49, No. 1, March 2014.

Itasca Consulting Group, Inc. 2016. *3DEC – 3-Dimensional Distinct Element Code, Ver. 5.2*. Minneapolis: Itasca.

Pells, P.J.N., Mostyn, G. & Walker, B.F. 1998. Foundations on Sandstone and Shale in the Sydney Region. *Australian Geomechanics Journal*, 33(3), pp.17-29.

Pells, P.J.N. 2004. Substance and Mass Properties for the Design of Engineering Structures in the Hawkesbury Sandstone. *Australian Geomechanics*. 39 (3): 1-21.